TRANSITION RADIATION OF RELATIVISTIC ELECTRONS FROM THE INTERPLANETARY SHOCK

K.S. MUSATENKO, I.O. ANISIMOV

UDC 533.9.01

Taras Shevchenko Kyiv National University, Faculty of Radiophysics
(6, Academician Glushkov Ave., Kyiv 03127, Ukraine; e-mail: ksm@univ.kiev.ua)

The model of the transition radiation from an electron drifting through the interplanetary shock region is suggested to explain CLUSTER and WIND multisatellite measurements. A wave equation for the longitudinal component of the vector-potential is obtained. Transition radiation patterns for the Fourier harmonics of the Poynting flux are presented. Properties of the radiation that appears in the considered system are discussed.

1. Introduction

The calculation and analysis of a transition radiation are related to different topics of applied physics, such as the development of particle detectors in nuclear physics [1], investigation of the radiation of modulated electron beams in active experiments in the ionosphere [2–4], and study of natural radiation sources, e.g., the solar radiation and the Earth's radiation in the km range [5–7]. Non-resonant transition radiation is commonly considered ineffective [1]. This conclusion is correct if a charged particle passes the inhomogeneity region only once. The radiation efficiency can be considerably increased in the case of multiple passages. This approach was used in [8], where a transition radiation mechanism was suggested to bring the signal out of a beam-plasma amplifier. In this article, we calculate the non-resonant transition radiation of a relativistic electron performing multiple rotations in the inhomogeneity region while crossing an interplanetary shock. The theoretical model that corresponds well to real experiment conditions is considered, and the results of calculations of the transition radiation within this model are presented.

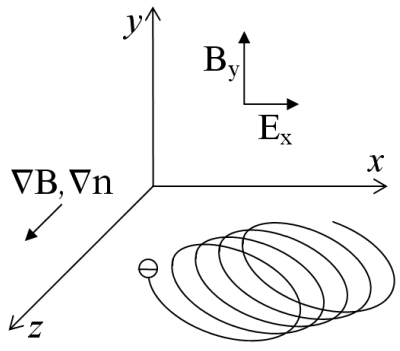

Fig. 1. Region of the interplanetary quasiperpendicular shock: the configuration of fields, gradients, and electron drift trajectory (schematic plot)

2. January 22, 2004 Interplanetary Shock Parameters and Theoretical Model

CLUSTER and WIND satellites performed *in situ* measurements of the strong electromagnetic emission at the frequency $1.4 - 1.6 f_{pe}$ [9] in the vicinity of the interplanetary quasiperpendicular shock crossing. In the same region, there was detected simultaneously the increased density of relativistic electrons. The authors of [9] suggested the transition radiation underlies a possible mechanism of the generation of electromagnetic waves.

The interplanetary shock on January 22, 2004 [9] was quasiperpendicular and supercritical with the Mach number $M_A \sim 5.6$; the shock ramp width could be resolved down to 150 km; the ratios of downstream to upstream magnetic field and density values were about 3.8. Relativistic electrons' trajectories in the vicinity of the shock front are driven by the constant component of the magnetic field, i.e. the cyclotron rotation (Fig. 1), gradient drift with the velocity $(2 \div 3) \times 10^4$ km/s, and $\vec{E} \times \vec{B}$-drift with the solar wind velocity. These drift velocities are significantly smaller than the full electron velocity $(0.5 \div 0.8)c$, where c is the velocity of light.

The interplanetary shock in the event on January 22, 2004 had the velocity of 740*[0.9; –0.3; 0.3] km/s GSE [10]. The average solar wind velocity at the bow shock nose was about 550–600 km/s [11]. Assuming that relativistic electrons detected by CLUSTER satellites were drifting with the solar wind velocity downstream, the relative velocity of the drift in the shock reference frame can be estimated as 150–200 km/s. The time of the electron presence in the inhomogeneity region of about one second allows the particle to perform few hundreds of cyclotron rotations with a period of 3–8 ms. The transition radiation occurs

every time when the particle crosses the inhomogeneity region. Therefore, even the non-resonant transition radiation can be quite effective.

In the measurements [9], the electron Larmor radius R_L was about hundreds of kilometers, and the length of the formation zone of transition radiation [1] was about few tens of kilometers. The cyclotron frequency of the electron rotation ω_c was several orders smaller than the local electron plasma frequency ω_p, that was, in turn, few times smaller than the electromagnetic emission frequency ω. In this case, the influence of a magnetic field on the dielectric permittivity can be neglected, and the role of the magnetic field consists only in the formation of the curvilinear trajectories of electrons. Thus, we come to the model of an electron having a quite complicated trajectory in the weakly inhomogeneous isotropic plasma.

The velocity of the guiding center is much smaller than the velocity of the electron cyclotron rotation. Therefore, as the first approximation, one can suggest the model of an electron having the circular orbit with the center that changes slowly its position along the linear positive density gradient. The transition radiation will exist all the time while the guiding center is situated in the inhomogeneity region, and its properties will change slowly as well.

As the first step, we consider the model of a relativistic electron rotating around the motionless center in a plasma with linear density profile, by neglecting the influence of a magnetic field on the dielectric permittivity (Fig. 2).

3. Wave Equation for Vector-potential and Its Solution

It is convenient to expand the current density of the rotating electron into plane waves. The transition radiation can be found for one plane wave of the current. Then the integration of all waves constituting the spectrum gives the total radiation intensity. According to the model under consideration, the electron has a circular orbit and rotates in the $x0z$ plane (Fig. 2). Thus, its motion can be described by the following dependences of coordinates on time:

$$x_\sim(t) = R_L \cos\omega_c t, \quad y_\sim(t) = 0, \quad z_\sim(t) = R_L \sin\omega_c t.$$

The corresponding velocity components can then be written as

$$\begin{cases} v_x(t) = -\omega_c R_L \sin\omega_c t, \\ v_z(t) = \omega_c R_L \cos\omega_c t, \end{cases}$$

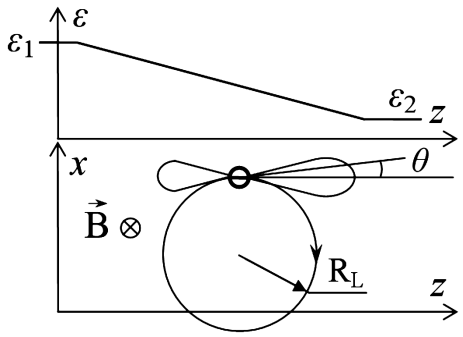

Fig. 2. Model of an electron having a rotating trajectory in plasma with linear density gradient (schematic plot)

and the current density created by one electron is

$$\vec{j}(\vec{r},t) = e(\vec{e_x}v_x + \vec{e_z}v_z)\delta(\vec{r} - \vec{r}(t)) =$$

$$= e(\vec{e_x}v_x + \vec{e_z}v_z)\delta(x - x(t))\delta(y(t))\delta(z - z(t)).$$

The expansions into the Fourier integral with respect to coordinates and the Fourier series in the time allow us to represent the full current density as a sum of plane waves:

$$j_x(\vec{k},t) = iC \sum_{n=-\infty}^{n=\infty} e^{in\omega_c t} B_{nx}(k_x,\kappa),$$

$$j_z(\vec{k},t) = C \sum_{n=-\infty}^{n=\infty} e^{in\omega_c t} B_{nz}(k_x,\kappa),$$

where coefficients C and $B_{nx,nz}$ are given by the expressions

$$C = \omega_c e R_L / 2(2\pi)^3;$$

$$B_{nx,nz}(k_x,\kappa) = J_{n-1}\left(R_L\sqrt{{k_x}^2 + \kappa^2}\right) e^{i(n-1)\arctan(k_x/\kappa)} \mp$$

$$\mp J_{n+1}\left(R_L\sqrt{{k_x}^2 + \kappa^2}\right) e^{i(n+1)\arctan(k_x/\kappa)}.$$

For the sake of simplicity, it is convenient to use the vector-potential $\vec{A}$ instead of the electric and magnetic fields. Then the wave equation for the vector-potential looks as

$$\text{grad div}\vec{A} - \Delta\vec{A} = \frac{4\pi}{c}\vec{j} + \epsilon k_0^2 \vec{A}, \qquad (1)$$

where $\epsilon(z) = \epsilon_1 + (\epsilon_2 - \epsilon_1)z/L$ is the dielectric permittivity, ϵ_1 and ϵ_2 are values of the dielectric permittivity upstream and downstream the shock. The dependence on time is taken as $exp(i\omega t)$ and $k_0 = \omega/c$.

As far as the model contains a chosen direction, it is natural to decompose the physical magnitudes into components parallel and perpendicular to the density gradient:

$$\vec{A} = \vec{e_z}A_{\parallel} + \vec{A_{\perp}}; \quad \vec{j} = \vec{e_z}j_{\parallel} + \vec{j_{\perp}}; \quad \vec{k} = \vec{e_z}k_z + \vec{k_{\perp}}.$$

Considering $\vec{A}(\vec{r}) = \vec{A}(z)\exp[-i(k_x x + k_y y)]$, Eq. (1) yields the wave equation for $A_{\parallel}$ that represents the electromagnetic wave excitation by a plane wave of current density:

$$A''_{\parallel zz} + \frac{\epsilon'_z}{\epsilon}A'_{\parallel z} + (\epsilon k_0^2 - k_{\perp}^2)A_{\parallel} =$$

$$= \frac{4\pi}{c\epsilon k_0^2}[(\kappa^2 - \epsilon k_0^2)j_{\parallel} + \kappa(\vec{k_{\perp}}\vec{j_{\perp}})]. \qquad (2)$$

According to measurements, the frequency of the detected electromagnetic radiation was quite different from the plasma frequency. Consequently, there was no point of local plasma resonance on the dielectric permittivity profile $\epsilon(z)$, and there was no reflection point for electromagnetic waves for reasonable values of $k_{\perp}$. Therefore, the solution of Eq. (1) can be found, by using the WKB approximation. This approximation is applicable only if the condition $2\pi/k_z \ll L$ is satisfied. In other words, the result obtained has physical sense only for angles with $\cos\theta \gg 2\pi/(k_{1,2}L)$, where θ is the angle between the radiation direction and the $0z$ axis, and subscripts correspond to the plasma upstream and downstream the shock (Fig. 2). Equation (2) is linear and non-uniform, thus its solution is a sum of an arbitrary partial solution of the non-uniform equation and a general solution of the uniform equation. The solution of the correspondent uniform equation in the WKB approximation consists of two terms corresponding to forward and backward waves with regard to the density gradient direction:

$$A_{\parallel}(z) = \frac{1}{\sqrt{\epsilon k_z}}(C_1 e^{i\psi(z)} + C_2 e^{-i\psi(z)}), \qquad (3)$$

where $\psi(z) = \int^z k_z(z')dz' = \int^z \sqrt{\epsilon(z')k_0^2 - k_{\perp}^2}dz'$ is the eikonal.

There is a plane wave of current density $j \sim \exp(-i\kappa z)$ on the right-hand side of Eq. (2). Therefore, it is natural to look for its partial solution describing the electric field of this current wave in the form

$$A_{\parallel}(z) = B(z)\exp(-i\kappa z).$$

The dependence $B(z)$ specified by a medium inhomogeneity is given by the expression

$$B(z) = \frac{i\exp(-i\Phi(z))}{\sqrt{\epsilon(z)}}\int^z \frac{f(z')}{2\kappa\sqrt{\epsilon(z')}}\exp[i\Phi(z')]dz',$$

where $f(z)\exp(-i\kappa z)$ is the right-hand side of Eq. (2), and $\Phi(z) = \int^z((k_z^2 - \kappa^2)/2\kappa)dz'$. Introducing the dependence of the WKB amplitudes on the coordinates [12], one can investigate the wave interaction in an inhomogeneous medium. Then the solution of Eq. (2) has a form

$$A_{\parallel}(z) = \frac{C_1(z)}{\sqrt{\epsilon(z)k_z(z)}}e^{i\psi(z)} + \frac{C_2(z)}{\sqrt{\epsilon(z)k_z(z)}}e^{-i\psi(z)} +$$

$$+B(z)\exp(-i\kappa z).$$

Substituting this solution in (2) and imposing the additional condition on the relation between C_1 and C_2 [12], we obtain the equation set that can be solved for the derivatives of the amplitudes $C_1(z)$ and $C_2(z)$:

$$\begin{cases} C'_{1z}(z) = \frac{\epsilon'_z}{4\epsilon}C_1(z) + \frac{1}{2}(\frac{k'_z}{k_z} + \frac{\epsilon'_z}{2\epsilon_z})C_2(z)e^{-i2\psi} + \\ +\frac{i}{2}\sqrt{\frac{\epsilon}{k_z}}B''_{zz}(z)e^{-i\kappa z - i\psi}, \\ C'_{2z}(z) = \frac{\epsilon'_z}{4\epsilon}C_2(z) + \frac{1}{2}(\frac{k'_z}{k_z} + \frac{\epsilon'_z}{2\epsilon_z})C_1(z)e^{i2\psi} - \\ -\frac{i}{2}\sqrt{\frac{\epsilon}{k_z}}B''_{zz}(z)e^{-i\kappa z + i\psi}. \end{cases} \qquad (4)$$

The first two terms on the right-hand sides of system (4) describe the mutual transformation of the forward and backward wave amplitudes. The last terms describe the transformation of the electric field current wave into the electromagnetic radiation. The integration of these terms by all inhomogeneity widths L allows us to compute the forward and backward transition radiations of a given current wave:

$$C_{1,2} = \pm\frac{i}{2}\int_0^L \sqrt{\frac{\epsilon(z')}{k_z(z')}}B''_{zz}(z')e^{-i\kappa z' \pm i\psi(z')}dz'. \qquad (5)$$

The calculation of that integral in the WKB approximation for the radiation on the n-th harmonic of the cyclotron frequency gives

$$C_{n1,2} = \frac{iC\pi(\epsilon_{n1} - \epsilon_{n2})}{c\kappa L}\times$$

$$\times e^{i(n\omega_c t \mp \int_0^0 k_z dz')}(e^{\mp i\int_0^L k_z dz'}D(L) - D(0)), \qquad (6)$$

where

$$D(z)=\frac{(\kappa^2-\epsilon_n(z)k_0^2)B_{nz}-i\kappa k_xB_{nx}}{k_z^{3/2}(z)(\kappa^2-k_z^2(z))}.$$

For further calculations, it is convenient to perform the transformation to a spherical coordinate system taking into account that

$$\epsilon(0)=\epsilon_1,\quad \epsilon(L)=\epsilon_2,\quad k_{1,2}=k_0\sqrt{\epsilon_{1,2}},$$

$$k_x=k\cos\phi_k\sin\theta_k,\quad k_y=k\sin\phi_k\sin\theta_k,\quad k_z=k\cos\theta_k,$$

$$k_x^2+k_y^2=k^2\sin^2\theta_k,\quad r=\sqrt{x^2+y^2+z^2},$$

$$x=r\cos\Phi_r\sin\Theta_r,\quad y=r\sin\Phi_r\sin\Theta_r,\quad z=r\cos\Theta_r.$$

The angles θ_k and ϕ_k indicate the wave vector direction, whereas Θ_r and Φ_r indicate the direction to a measurement point. Then expression (6) can be rewritten as

$$C_{n1,2}=\frac{iC\pi(\epsilon_{n1}-\epsilon_{n2})}{c\kappa L}(\exp(\mp\frac{i3k_0\cos\theta_kL}{2(\epsilon_{n1}-\epsilon_{n2})}\epsilon_{n2}^{3/2})\times$$

$$\times\frac{(\kappa^2-\epsilon_{n2}(z)k_0^2)B_{nz}-i\kappa\sqrt{\epsilon}_{n1,2}k_0\cos\phi_k\sin\theta_kB_{nx}}{(\sqrt{\epsilon}_{n2}k_0\cos\theta_k)^{3/2}(\kappa^2-(\sqrt{\epsilon}_{n2}k_0\cos\theta_k)^2(z))}-$$

$$-\left(\exp\left(\mp\frac{i3k_0\cos\theta_kL}{2(\epsilon_{n1}-\epsilon_{n2})}\epsilon_{n1}^{3/2}\right)\times\right.$$

$$\left.\times\frac{(\kappa^2-\epsilon_{n1}(z)k_0^2)B_{nz}-i\kappa\sqrt{\epsilon}_{n1,2}k_0\cos\phi_k\sin\theta_kB_{nx}}{(\sqrt{\epsilon}_{n1}k_0\cos\theta_k)^{3/2}(\kappa^2-(\sqrt{\epsilon}_{n1}k_0\cos\theta_k)^2(z))}\right).$$

The vector-potentials of forward and backward radiations for one plane wave of current are given by the expression

$$A_{\parallel n1,2}(z)=\frac{C_{n1,2}(z)}{\sqrt{\epsilon_{n1,2}(z)k_{z1,2}(z)}}e^{-i(k_xx+k_yy\mp k_zz)}. \qquad (7)$$

Consequently, the inverse Fourier transformation with respect to k_x and k_y gives

$$A_{\parallel n1,2}(z)=\int\limits_{-\infty}^{\infty}dk_x\int\limits_{-\infty}^{\infty}dk_y\frac{C_{n1,2}(z)e^{-i(k_xx+k_yy\mp k_zz)}}{\sqrt{\epsilon_{n1,2}(z)k_{z1,2}(z)}}=$$

$$=-k_{1,2}^2\frac{iC\pi(\epsilon_{n1}-\epsilon_{n2})}{c\kappa L}\int\limits_0^{2\pi}d\phi_k\int\limits_0^{\pi}\sin2\theta_kd\theta_k\times$$

$$\times\frac{\exp(-ik_{1,2}r(\sin\Theta_r\sin\theta_k\cos(\Phi_r-\phi_k)\mp\cos\Theta_r\cos\theta_k))}{\sqrt{\epsilon_{n1,2}(z)k_{1,2}(z)\cos\theta_k}}\times$$

$$-(\exp(\mp\frac{i3k_0\cos\theta_kL}{2(\epsilon_{n1}-\epsilon_{n2})}\epsilon_{n2}^{3/2})\times$$

$$\times\frac{(\kappa^2-\epsilon_{n2}(z)k_0^2)B_{nz}-i\kappa\sqrt{\epsilon}_{n1,2}k_0\cos\phi_k\sin\theta_kB_{nx}}{(\sqrt{\epsilon}_{n2}k_0\cos\theta_k)^{3/2}(\kappa^2-(\sqrt{\epsilon}_{n2}k_0\cos\theta_k)^2)}-$$

$$-(\exp(\mp\frac{i3k_0\cos\theta_kL}{2(\epsilon_{n1}-\epsilon_{n2})}\epsilon_{n1}^{3/2})\times$$

$$\times\frac{(\kappa^2-\epsilon_{n1}(z)k_0^2)B_{nz}-i\kappa\sqrt{\epsilon}_{n1,2}k_0\cos\phi_k\sin\theta_kB_{nx}}{(\sqrt{\epsilon}_{n1}k_0\cos\theta_k)^{3/2}(\kappa^2-(\sqrt{\epsilon}_{n1}k_0\cos\theta_k)^2)}),(8)$$

where it was taken into account that

$$dk_xdk_y=-k^2\sin2\theta_kd\phi_kd\theta_k,$$

$$k_xx+k_yy\mp k_zz=$$

$$=kr(\sin\Theta_r\sin\theta_k\cos(\Phi_r-\phi_k)\mp\cos\Theta_r\cos\theta_k).$$

Integrals (8) can be calculated using the stationary phase method in the far zone ($k_{1,2}r\gg1$). The stationary phase points for integrals over ϕ_k and θ_k correspond to the direction to the measurement point: $\phi_k=\Phi_r$ and $\theta_k=\Theta_r$. In this way, we come to the relation

$$A_{\parallel n1,2}=-k_{1,2}\frac{i4C\pi^2(\epsilon_{n1}-\epsilon_{n2})}{cLr}\frac{\cos\Theta_r}{\sqrt{|\cos2\Theta_r|}}\times$$

$$\times\frac{\exp(-ik_{1,2}r(i\pi/4(\delta_{S''\phi}+\delta_{S''\theta})-\cos2\Theta_r))}{\sqrt{\epsilon_{n1,2}(z)k_{1,2}(z)\cos\Theta_r}}\times$$

$$\times\int\limits_{-\infty}^{\infty}d\kappa\Big(\exp(\mp\frac{i3k_0\cos\Theta_rL}{2(\epsilon_{n1}-\epsilon_{n2})}\epsilon_{n2}^{3/2})\times$$

$$\times\frac{(\kappa^2-k_2^2)B_{nz}-i\kappa k_2\cos\Phi_r\sin\Theta_rB_{nx}}{(k_2\cos\Theta_r)^{3/2}\kappa(\kappa^2-(k_2\cos\Theta_r)^2)}-$$

$$-\exp(\mp\frac{i3k_0\cos\Theta_rL}{2(\epsilon_{n1}-\epsilon_{n2})}\epsilon_{n1}^{3/2})\times$$

$$\times\frac{(\kappa^2-k_1^2)B_{nz}-i\kappa k_1\cos\Phi_r\sin\Theta_rB_{nx}}{(k_1\cos\Theta_r)^{3/2}\kappa(\kappa^2-(k_1\cos\Theta_r)^2)}\Big). \qquad (9)$$

The integration over κ is performed via numerical methods. The largest contribution to integral (9) is made by the Cherenkov resonance region, where $\kappa=\pm k_{1,2}\cos\Theta_r$.

Given the amplitude of the vector-potential longitudinal component harmonic $A_{\parallel n1,2}$, we can obtain the radial component of the Poynting vector:

$$\Pi_{Rn1,2}=\frac{c\sqrt{\epsilon}}{4\pi}E_{\Theta_r}^2=$$

$$=\frac{n^2\omega_c^2}{c}\frac{\sqrt{\epsilon}_{n1,2}}{4\pi}\Big(\frac{\sin^2\Theta_r\mp\cos^2\Theta_r}{\sin\Theta_r}\Big)^2A_{\parallel n1,2}^2.$$

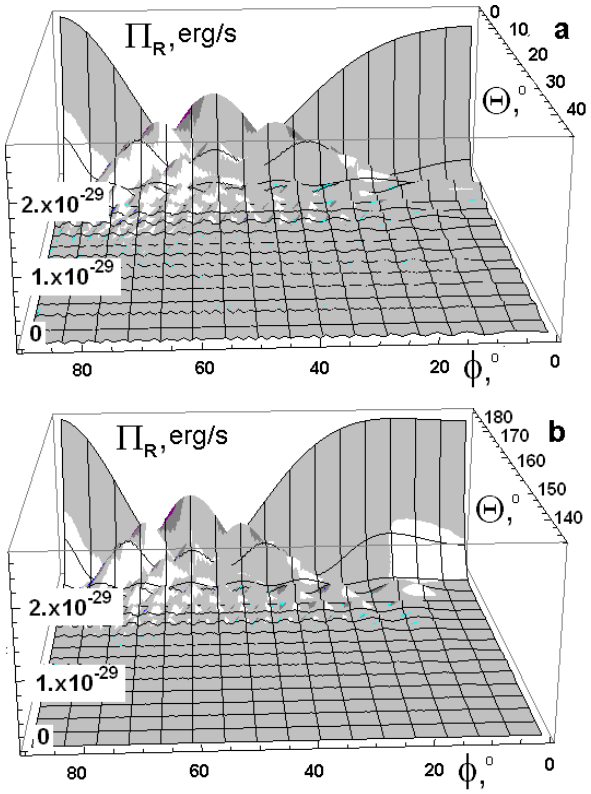

Fig. 3. Forward (a) and backward (b) radiation patterns for the $n = 250$ harmonic of the Poynting flux radial component in the far zone for the relativistic electron with the energy $E_e = 300$ keV in a plasma with the upstream and downstream densities $n_1 = 1{\times}10^5$ m^{-3} and $n_2 = 2.2{\times}10^5$ m^{-3}, the magnetic field $B = 16{\times}10^{-9}$ T, and the inhomogeneity scale $L = 1.5{\times}10^5$ m

4. Preliminary Results and Discussion

We assume that the forward radiation propagates in the angle range $0 < \theta < \pi/2$, and the backward radiation propagates in the angle range $\pi/2 < \theta \leq \pi$ (Fig. 3). As far as the forward radiation propagates into the plasma with a smaller dielectric permittivity value, it comes out of the shock region at all possible angles between 0 and $\pi/2$. The backward radiation is emitted into the plasma with a higher value of refraction index. Therefore, it will exist only for angles satisfying the inequality $\theta \geq \pi - \arcsin(\sqrt{\epsilon_2/\epsilon_1})$.

The typical forward and backward transition radiation patterns created by a given partial wave of current density are presented in Fig. 3. Due to the reasons described above, these patterns make sense only in the limited range of the angle θ.

It can be seen from Fig. 3 that the directivity diagram of the Poynting flux harmonic has oscillating structure. Probably, it is a result of the interference pattern that is formed in the far zone by the radiation from different electron spatial locations. Indeed, the wave length of the measured radiation is about 3–4 m, while the trajectory scale can be estimated as the Larmor radius ~ 100 km.

Usually, relativistic electrons generate the transition radiation that propagates mostly at small angles to the velocity direction [1]. In the case of a straight trajectory, this results into a more intense forward radiation. In the suggested model, the relativistic electron is rotating. Consequently, the transition radiation calculation gives forward and backward radiation powers of the same order.

The transition radiation Poynting flux for one Fourier harmonic obtained for the chosen model gives the result exceeding considerably that obtained for the straight electron propagation. For example, the transition radiation for the $n = 250$ harmonic is by more than 80 orders of magnitude higher than that in the case of a straight trajectory [1]. Thus, the electron rotation provides a much higher radiation efficiency.

5. Conclusions

Properties of the transition radiation under study can be described as follows.

1. Forward and backward transition radiations of the relativistic electron drifting through the interplanetary shock region are of the same order.

2. Both the forward and backward radiation patterns have highly oscillating structure due to the interference observed in the far zone from different electron locations.

3. The transition radiation of the relativistic electron having circular orbit is much higher than that obtained for the straight electron propagation.

The preliminary results of this work are outlined in [13–16].

1. V.L. Ginzburg, V.N. Tsytovich, *Transition Radiation and Transition Scattering* (Nauka, Moscow, 1984) (in Russian).

2. D.G. Cartwright and P.J. Kellog, J. Geophys. Res. **79**, 1439 (1974).

3. V.A. Balakirev, V.A. Buts, V.I. Kurilko, Zh. Tekhn. Fiz. **46**, 477 (1976).

4. A.V.Kostrov, M.A.Starodubtsev, C.Krafft, G.Mattihieussent, and A.S.Volokitin in *Abstracts of Invited and Contributed Papers of International Congress on Plasma Physics*, Prague, 1998, edited by J. Badalec, J. Stokel, P. Sunka, M. Tendler, Part III, p.152.

5. V.V. Zheleznyakov, *Radioemission of the Sun and Planets* (Nauka, Moscow, 1964) (in Russian).

6. E.N. Ermakova and V.Yu. Trakhtengerts, Geomag. Aeronom. **21**, 82 (1981).
7. A.G. Boev and M.Yu. Luk'yanov, Astron. Zh. **68**, 853 (1991).
8. I.O.Anisimov, S.M.Levytsky and S.M.Myshko, Ukr. Phys. J. **49**, 1087 (2004).
9. Yu. Khotyaintsev, V. Krasnoselskikh, M.V. Khotyaintsev, and S. Mühlbachler, in *Abstract book of the 2nd Conference on Spatio-Temporal Analysis and Multipoint Measurements in Space*, Orleans, 2007, p. 37.
10. A.N. Fazakerley *et al.*, Geophys. Res. Lett. **32**, L13105, doi: 10.1029/2005GL0022842, (2005).
11. Space Physics Data Facility, http://omniweb.gsfc.nasa.gov/, Goddard Space Flight Center.
12. M.I. Rabinovich, D.S. Trubetskov, *Introduction into the Theory of Oscillations and Waves* (Nauka, Moscow, 1984) (in Russian).
13. K.S. Musatenko, I.O. Anisimov, and V.V. Krasnoselskikh, in *Proceedings of the Seventh International Young Scientists Conference on Applied Physics*, Kyiv, 2007, p. 144.
14. K.S. Musatenko, I.O. Anisimov, and V.V. Krasnoselskikh, in *Abstracts of the Ukrainian Conference on Plasma Physics and Controlled Fusion – 2007*, Kyiv, 2007, p. 63 (in Russian).
15. K.S. Musatenko, I.O. Anisimov, and V.V. Krasnoselskikh, in *Abstracts of the 2nd Conference on Spatio-Temporal Analysis and Multipoint Measurements in Space*, Orleans, 2007, p. 41.
16. K.S. Musatenko, I.O. Anisimov, and V.V. Krasnoselskikh, in *Proceedings of the Third International Conference 'Electronics and Applied Physics'*, Kyiv, 2007, p. 130.

ПЕРЕХІДНЕ ВИПРОМІНЮВАННЯ РЕЛЯТИВІСТСЬКИХ ЕЛЕКТРОНІВ З МІЖПЛАНЕТНОЇ УДАРНОЇ ХВИЛІ

К.С. Мусатенко, І.О. Анісімов

Р е з ю м е

Для пояснення багатосупутникових вимірювань CLUSTER та WIND запропоновано модель перехідного випромінювання релятивістського електрона, що дрейфує через область міжпланетної ударної хвилі. Отримано хвильове рівняння для поздовжньої компоненти вектор-потенціалу. Наведено діаграми напрямленості фур'є-гармоніки вектора Пойнтінга. Обговорено властивості випромінювання, що виникає в такій системі.